Supporting Information for

Site selective substitution and its influence on photoluminescence properties of Sr0.8Li0.2Ti0.8Nb0.2O3 :Eu3+ phosphors

G.Jyothi; L.Sandhya Kumari; K.G.Gopchandran *

Department of Optoelectronics, University of Kerala, Thiruvananthapuram-695581, India.

*gopchandran@yahoo.com

Calculation procedure for Judd-Ofelt intensity parameters

The magnetic dipole transition rate is calculated using the equation,

$$A_{01} = \frac{64\pi^4 n^3 \nu_1^3 S_{md}}{3h(2J+1)} \tag{1}$$

where ν_1 is the wave number of emission corresponding to the transition.

The values of Ω_2 and Ω_4 are determined using the relations,

$$\frac{A_{0J}}{A_{01}} = \frac{e^2 {\nu_J}^3 (n^2+2)^2}{9 S_{md} \nu_1^3 n^2} \Omega_\lambda \left| < {}^5D_0 \| U^{(\lambda)} \| {}^7F_J > \right|^2 \tag{2}$$

and

$$\frac{A_{0J}}{A_{01}} = \frac{\int I_J d\nu}{\int I_1 d\nu} \tag{3}$$

where $\int I_J d\nu$ is the integrated emission intensity of ${}^5D_0 \rightarrow {}^7F_J$ transition.

Figure S1 (a) XRD patterns and (b) expanded view of (110) reflection of $Sr_{0.95-x}Eu_{0.05}Li_xTi_{1-x}Nb_xO_3$ phosphors.

Figure S2 Raman spectra of (a) SL_1:$Sr_{0.8-x}Li_{0.2}Ti_{0.8}Nb_{0.2}O_3$:$xEu^{3+}$ and (b) SL_2: $Sr_{0.8-x/2}Li_{0.2}Ti_{0.8-x/2}Nb_{0.2}O_3$:$xEu^{3+}$

Figure S3 The DR spectra and Inset: $[F(R_\alpha)h\nu]^2$ versus band gap plots of $SrTiO_3$ (ST), $Sr_{0.8}Li_{0.2}Ti_{0.8}Nb_{0.2}O_3$ (SL), $Sr_{0.68}Eu_{0.12}Li_{0.2}Ti_{0.8}Nb_{0.2}O_3$ (SL_1c) and $Sr_{0.74}Eu_{0.12}Li_{0.2}Ti_{0.74}Nb_{0.2}O_3$ (SL_2c).

Figure S4 Excitation spectra of different samples monitored at 615 nm (a) SL_1: $Sr_{0.8-x}Li_{0.2}Ti_{0.8}Nb_{0.2}O_3$:$xEu^{3+}$ and (b) SL_2: $Sr_{0.8-x/2}Li_{0.2}Ti_{0.8-x/2}Nb_{0.2}O_3$:$xEu^{3+}$

Figure S5 Emission spectra of SL_1: $Sr_{0.8-x}Li_{0.2}Ti_{0.8}Nb_{0.2}O_3$:$xEu^{3+}$ phosphors under (a) 465 nm and (b) 395 nm excitations

Figure S6 Emission spectra of SL_2:$Sr_{0.8-x/2}Li_{0.2}Ti_{0.8-x/2}Nb_{0.2}O_3$:$xEu^{3+}$ phosphors under (a) 465 nm and (b) 395 nm excitations; insets, the expanded view of $^5D_o \rightarrow {}^7F_1$ and $^5D_o \rightarrow {}^7F_2$ transitions for the respective excitations.

Figure S7 Emission spectra of $Sr_{0.95-x}Eu_{0.05}Li_xTi_{1-x}Nb_xO_3$ phosphors under 465 nm excitation

Figure S8 Emission spectra of $Sr_{0.8}Li_{0.2}Ti_{0.8}Nb_{0.2}O_3$:$Eu^{3+}$ phosphors in which Eu^{3+} substituted at Sr and Ti sites at different doping ratio, under 465 nm excitation.

Figure S9 The photoluminescence decay curves for $^5D_0 \rightarrow {}^7F_2$ transition (615 nm) of (a) $Sr_{0.8-x}Eu_xLi_{0.2}Ti_{0.8}Nb_{0.2}O_3$ (SL_1) phosphors and (b) $Sr_{0.8-x/2}Eu_xLi_{0.2}Ti_{0.8-x/2}Nb_{0.2}O_3$ (SL_2) phosphors under 465 nm excitation.

Table S1. Structural parameters of $Sr_{0.8-x}Li_{0.2}Ti_{0.8}Nb_{0.2}O_3$:x$Eu^{3+}$ (SL_1) and $Sr_{0.8-x/2}Li_{0.2}Ti_{0.8-x/2}Nb_{0.2}O_3$:x$Eu^{3+}$ (SL_2) phosphors.

Table S2. Band gap energy of $Sr_{0.8-x}Eu_xLi_{0.2}Ti_{0.8}Nb_{0.2}O_3$ (SL_1) and $Sr_{0.8-x/2}Eu_xLi_{0.2}Ti_{0.8-x/2}Nb_{0.2}O_3$ (SL_2) phosphors.

Figure S1

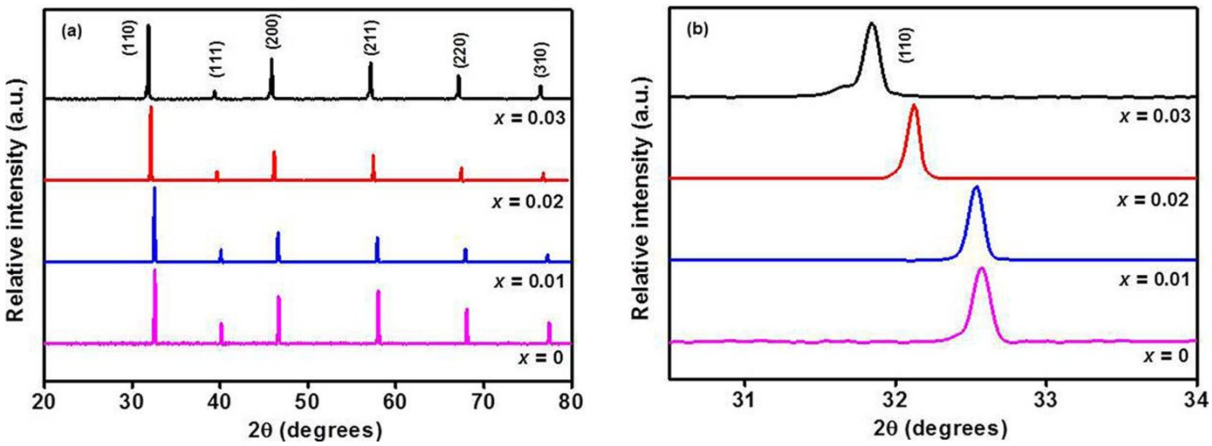

Figure S2

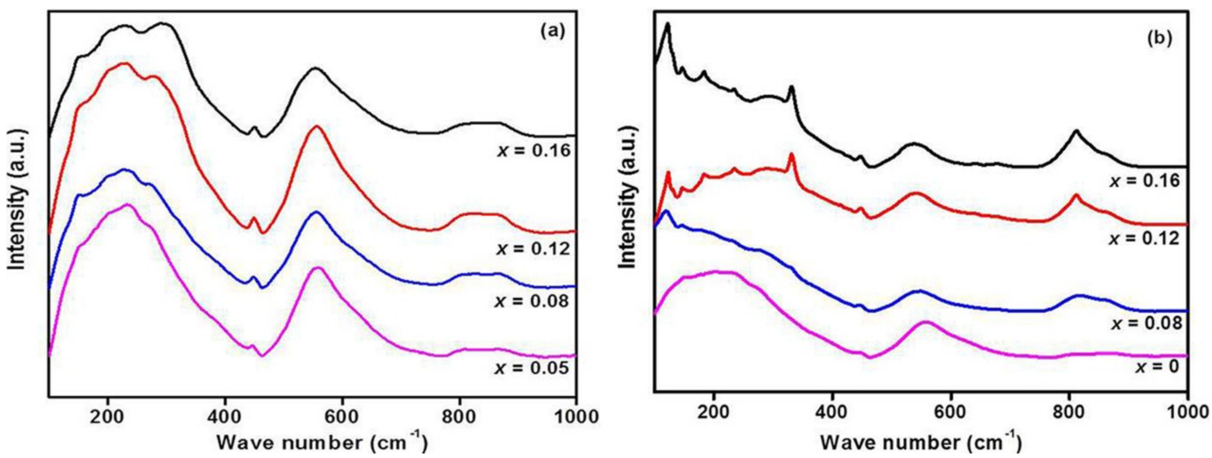

Figure S3

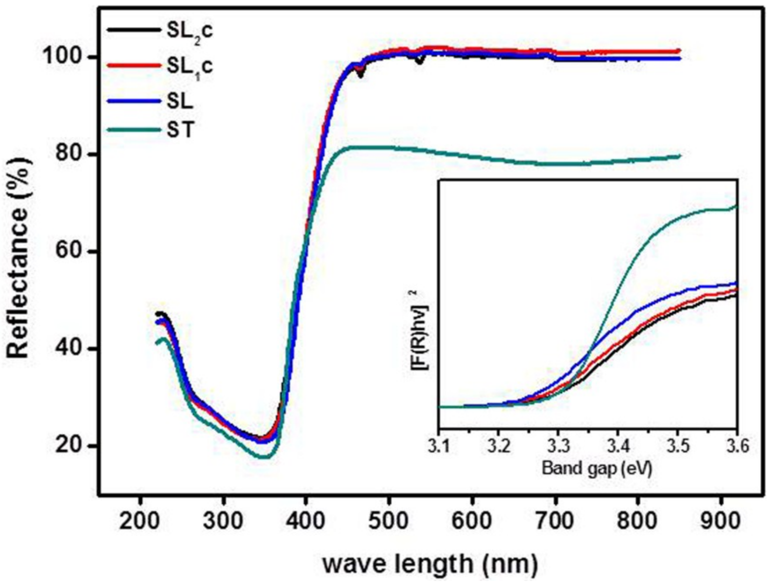

Figure S4

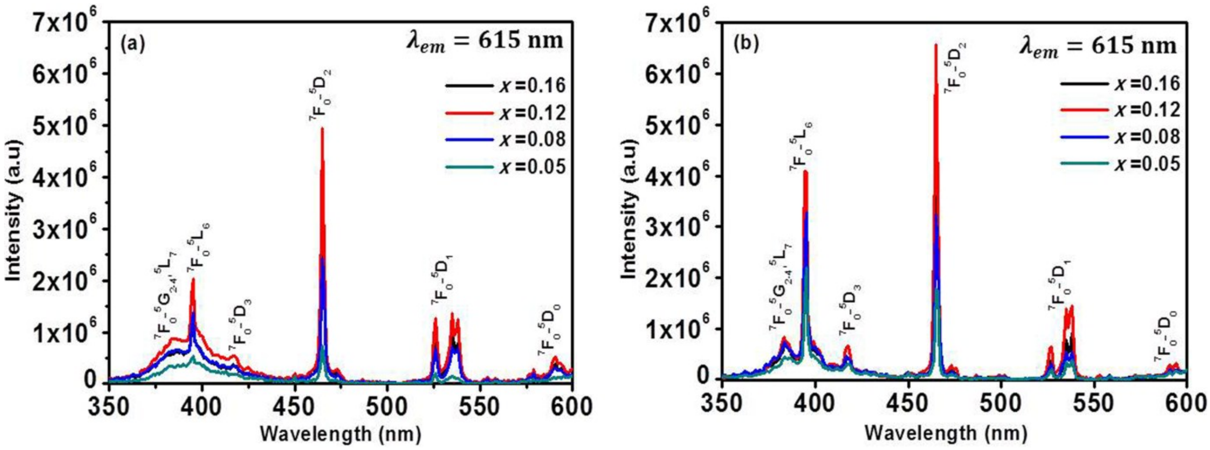

Figure S5

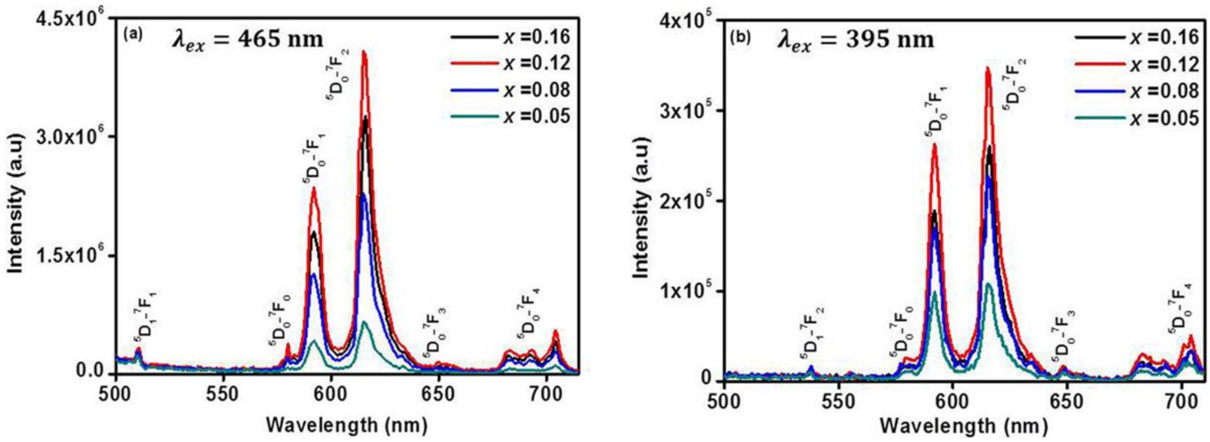

Figure S6

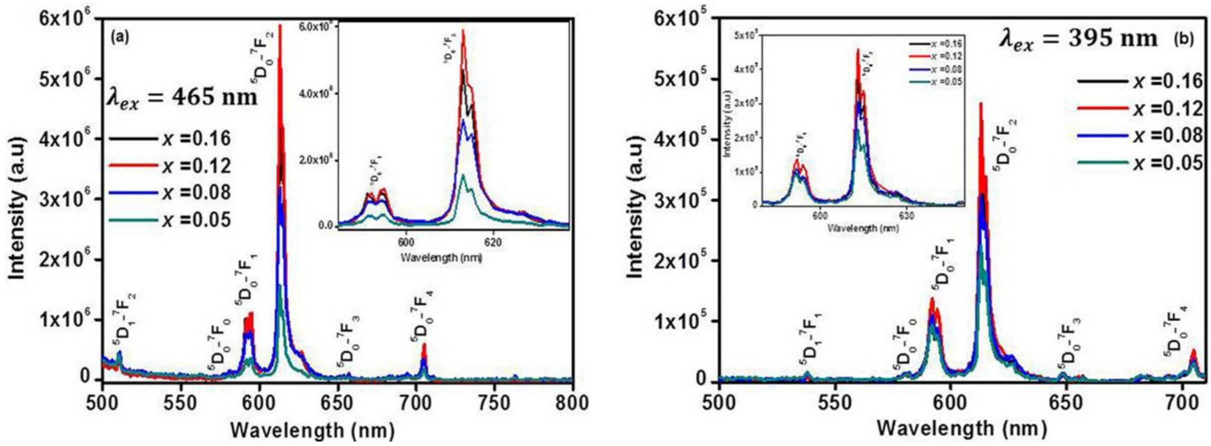

Figure S7

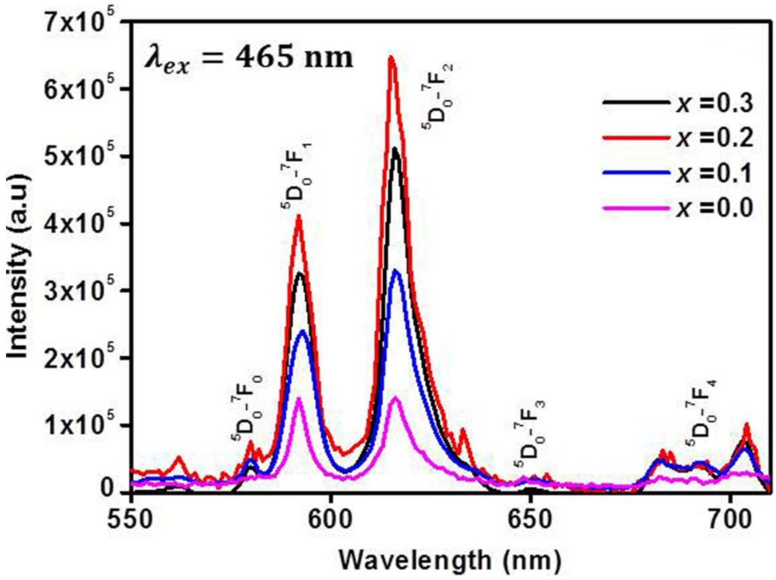

Figure S8

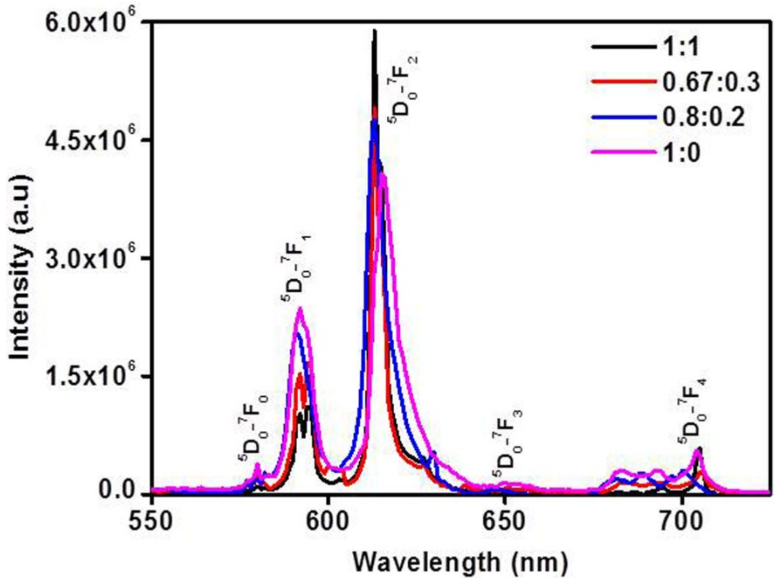

Figure S9

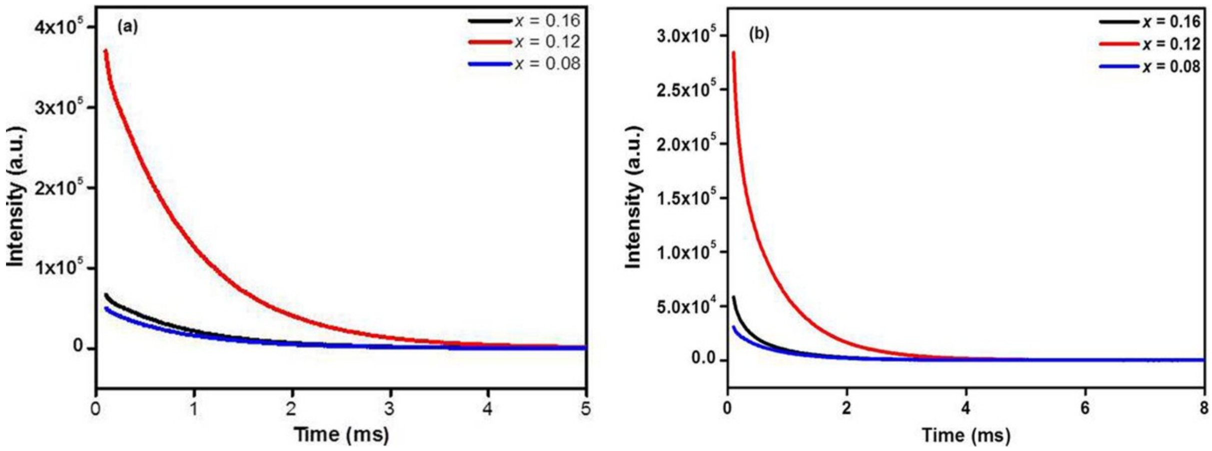

Table S1

Sample	SL1: $Sr_{0.8-x}Eu_xLi_{0.2}Ti_{0.8}Nb_{0.2}O_3$				SL2: $Sr_{0.8-x/2}Eu_xLi_{0.2}Ti_{0.8-x/2}Nb_{0.2}O_3$			
	x=0.05	*x*=0.08	*x*=0.12	*x*=0.16	*x*=0.05	*x*=0.08	*x*=0.12	*x*=0.16
a (Å)	3.9100(1)	3.9064(1)	3.9021(1)	3.9006(1)	3.9129(1)	3.91400(5)	3.9159(1)	3.9175(1)
Rp (%)	11.43	10.44	13.76	12.01	10.27	9.1	12.19	10.97
Rwp (%)	14.9	14.34	15.86	14.84	14.06	12.23	15.21	12.68
χ2 %	1.6	1.9	1.6	1.9	1.6	1.8	1.5	1.7
Sr-O (Å)	2.7650 (1)	2.7620 (1)	2.7590 (2)	2.7580 (2)	2.7670 (3)	2.7680 (1)	2.7690 (2)	2.7710 (1)
Ti-O (Å)	1.9550(1)	1.9530(1)	1.9510 (2)	1.9500 (2)	1.9560 (3)	1.9570 (1)	1.9580 (2)	1.9600(1)

Table S2

Value of x	Band gap (eV)	
	SL_1	SL_2
0	3.24	3.24
0.08	3.23	3.27
0.12	3.23	3.30
0.16	3.23	3.31